Impact of machine log-files uncertainties on the quality assurance of proton pencil beam scanning treatment delivery

Impact of machine log-files uncertainties on the quality assurance of proton pencil beam scanning treatment delivery

S. Toscano[1], K. Souris[2], C. Gomà[1,3], A. Barragan-Montero[2], S. Puydupin[4], F. Vander Stappen[4], G. Janssens[4], A. Matic[4], X. Geets[5], E. Sterpin[1,2].

[1] KU Leuven, Department of Oncology, Laboratory of Experimental Radiotherapy, Leuven, Belgium
[2] Université catholique de Louvain, Institut de Recherche Expérimentale et Clinique, Center of Molecular Imaging Radiotherapy and Oncology, Brussels, Belgium
[3] University Hospitals Leuven, Department of Radiation Oncology, Leuven, Belgium
[4] Ion Beam Applications, Louvain-la-Neuve, Belgium
[5] Department of Radiation Oncology, Cliniques universitaires Saint-Luc, Brussels, Belgium

E-mail: simona.toscano@kuleuven.be

Abstract

Irradiation log-files store useful information about the plan delivery, and together with independent Monte Carlo dose engine calculations can be used to reduce the time needed for patient-specific quality assurance (PSQA). Nonetheless, machine log-files carry an uncertainty associated to the measurement of the spot position and intensity that can influence the correct evaluation of the quality of the treatment delivery. This work addresses the problem of the inclusion of these uncertainties for the final verification of the treatment delivery.

Dedicated measurements performed in an IBA Proteus Plus gantry with a pencil beam scanning (PBS) dedicated nozzle have been carried out to build a "room-dependent" model of the spot position uncertainties. The model has been obtained through interpolation of the look-up tables describing the systematic and random uncertainties, and it has been tested for a clinical case of a brain cancer patient irradiated in a dry-run. The delivered dose has been compared with the planned dose with the inclusion of the errors obtained applying the model.

Our results suggest that the accuracy of the treatment delivery is higher than the spot position uncertainties obtained from the log-file records. The comparison in terms of DVHs shows that the log-reconstructed dose is compatible with the planned dose within the 95% confidence interval obtained applying our model. The initial mean dose difference between the calculated dose to the patient based on the plan and recorded data is around 1%. The difference is essentially due to the log-file uncertainties and it can be removed with a correct treatment of these errors.

In conclusion our new PSQA protocol allows for a fast verification of the dose delivered after every treatment fraction through the use of machine log-files and an independent Monte Carlo dose engine. Moreover, the inclusion of log-file uncertainties in the dose calculation allows for a correct evaluation of the quality of the treatment plan delivery.

Keywords: proton therapy, Monte Carlo simulation, machine log files, quality assurance.

1. Introduction

With the advent of pencil beam scanning (PBS), proton therapy treatments are becoming extremely flexible and complex. In intensity modulated proton therapy (IMPT) highly conformal dose distributions are achieved by means of thousands of individually and simultaneously optimised beamlets (Lomax 1999). Such a complex methodology requires the development of comprehensive protocols for patient-specific quality assurance (PSQA) of the treatment plan, to check for errors in the propagation of information from the treatment planning system (TPS) to the treatment machine and the plan delivery.

Current clinical PSQA workflows typically include cumbersome field-specific measurements in water such as two-dimensional (2D) dose distribution in the planes perpendicular to the incident beam direction for each field at multiple depths (Zhu et al 2011). The measured 2D-delivered dose at a chosen depth is compared to the planned dose generally using the gamma-index test (Low at al 1998). Such a methodology is far to be comprehensive and does not assure the quality of the full treatment plan. In addition, a PSQA based on measurements in water phantoms is time consuming or even prohibitive in view of the introduction of an adaptive scheme during proton therapy treatments, which would require additional verifications for every re-planning. For this reason, alternative solutions based on the so-called machine "log-files" have been proposed in several works published during the last years (Zhu et al 2015, Meier et al 2015, Scandurra et al 2016, Belosi et al 2017). Machine log-files include relevant information such as the position of the delivered spots and their intensity in terms of delivered monitor units (MU). This information used together with Monte Carlo computations can be used to assess the actual dose delivered to the patient during the full treatment.

A check on the actual plan can be afforded in a simple and fast way using the information from the data recorded by machine measurement devices during delivery. Unfortunately, measurements come with an associated uncertainty that may limit the potential of such a tool to evaluate the correctness of the treatment delivery, and lead to a biased estimation of the rate of acceptable plans. Therefore, the characterization of these uncertainties is of utmost importance and its impact on the reconstructed dose needs to be addressed. A model of the log-file uncertainties can be built with the help of dedicated measurements and can be easily incorporated in the calculation of the delivered dose in a Monte Carlo (MC) log-based PSQA. The aim of this work is to define a methodology to characterise and model the log-file uncertainties (LogQA), describing how the model is integrated in a more comprehensive and independent dose calculation system for PBS proton therapy.

2. Methods and materials

PSQA is recommended for PBS treatment delivery to verify the dose calculated by the TPS and the correctness of the treatment delivery. The new post-treatment MC log-based PSQA program is based on an independent in-house Monte Carlo dose engine, MCsquare (Souris et al 2016), which allows for a fast recalculation of the dose to the patient and is available as an open source tool. With MCsquare, a full treatment can be simulated in a few minutes.

2.1. Measurements and modelling of the log-file uncertainties

We compared the spot position measured by the treatment machine against the measurements performed with an external detector and the original plan to characterize the deviations of the log-file measurements from the actual delivery.

A dedicated experiment with a PBS proton beam was designed to explore the impact of the machine measurement uncertainties on the recorded spot positions. Measurements were

performed in an IBA Proteus Plus gantry with a PBS-dedicated nozzle. In a scanning gantry for proton therapy PBS treatment, as the IBA system in this work, the beam position is modified varying the current on the two magnets, used to scan the two orthogonal directions (x, y). The spot position and MU are measured through three ionization chambers (IC). The two latest ICs, placed after the scanning magnets, are composed of (respectively) horizontal and vertical strips to determine the spot position. While the MU is directly related to the charge read-out of the ICs (~3e-9 C for PBS dedicated nozzle), the spot position recorded in the machine log-files is the result of a three-point-based fast Gaussian fit, which carries an uncertainty expected to be greater than the precision of the scanning system after commissioning of the current in the magnets. The recorded spot positions are reported at the nozzle level, and converted to positions at the isocenter before any comparison with measurements can be made. This transformation takes into account the beam divergence of the PBS scanning system.

Proton beams were measured in air using the Lynx®, a 2d-scintillator based detector with CCD camera, with an active surface of 30x30 cm^2 and effective resolution of 0.5 mm, made by Fimel and distributed by IBA Dosimetry (Schwarzenbruck, Germany). All measurements were performed at the isocenter with the Lynx attached to the nozzle by means of a 50-cm metallic arm. A plumb was attached in front of the Lynx, and the existing X-ray system was used to produce a uniform radiation field detected by the Lynx. The rotation of the Lynx was corrected till the string projection had a rotation tilt smaller than 0.5 mm/m (0.125 mm/Lynx length). The isocentre coordinate on the Lynx was performed using X-rays and a metallic plate with four markers for correct positioning, reaching an accuracy of ± 0.5 mm. The main source of the error can be assigned to the Lynx accuracy to be up to 0.5 mm for its central region. The irradiated plan is a 20x20 cm^2 field with 25 spots equally separated at a distance of 5 cm, and a wide range of MUs and Energy (Energy = [100, 150, 200, 226.7] MeV, MU = [0.1, 0.5, 1, 5, 10]). Every combination of MU-Energy was irradiated 5 times and at two gantry angles (0˚, 270˚). Lynx measurements were performed meanwhile, only when the minimal dose received per spot allowed for a reliable reconstruction of the spot position. Considering the existing beam properties of the used gantry, this threshold was set to 0.5 MUs. The amount of light received by the CCD camera was modulated changing the aperture (IRIS) to avoid any saturation of the signal in the camera. Figure 1 shows two images of the irradiated spots obtained with the Lynx for 100 MeV and 226.7 MeV. As expected the spot size decreases with increasing energy.

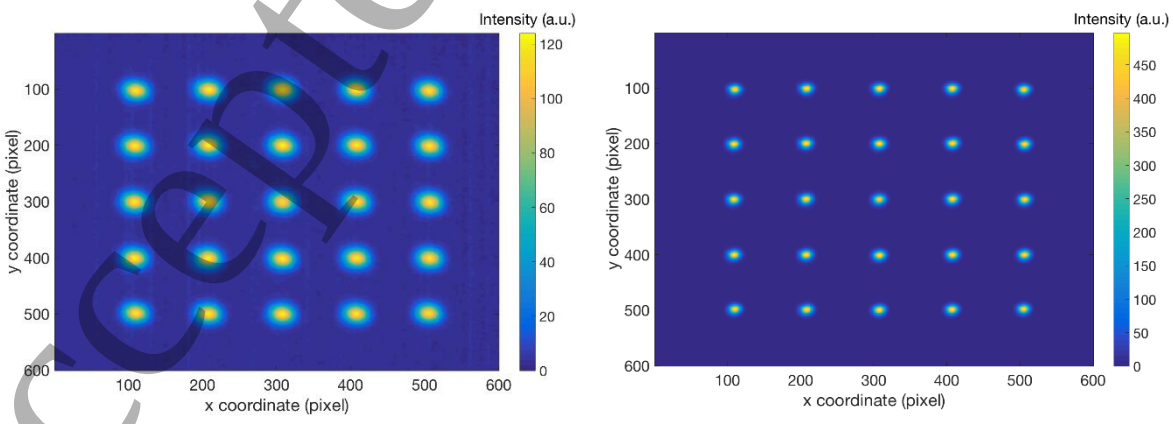

Figure 1 Lynx image of the delivered dose at MU = 0.5. The left panel shows the spots image at 100 MeV, while the right panel shows the spots image at 226.7 MeV.

The lack of measurement at MU < 0.5 requires separating the analysis in two intensity regions. Hereafter we will refer to *high-MUs* when MU >=0.5, and *low-MUs* when MU < 0.5.

2.1.1. Spot position reconstruction for *high-MUs*

As already mentioned, machine log-files record information about the irradiation of the treatment plan. In particular, the measured spot position and charge can be used to reconstruct the actual delivered plan. More in details, the read-out of the IC is performed every 250 μsec, a time stamp smaller than the delivery of a single spot, in such a way to have several measurements recorded for the same spot. We take the last measured spot position as the most accurate, since at every new time stamp the spot position is updated based on the integral charge since the beginning of the spot irradiation. The total charge is obtained by summing up the charge measured at every step (Figure 2).

We study the spot position difference between the log-recorded value and the Lynx measurement (our benchmark position). Being the measurements independent, according to the central limit theorem, we expect the difference to follow a Gaussian distribution, where the sigma represents the statistical or random uncertainty of the log-file measurement. In a case where no systematic uncertainty is present, we expect the Gaussian distribution to be centered at zero. Therefore the mean of the distribution gives an estimation of the log-file systematic error. Comparing the spot position recorded in the log-files with the position measured with the Lynx we can extract, in such a way, the systematic and random shift of the spot position as a function of several parameters (MU, Energy, spot position in the isocenter plane (x, y)).

2.1.2. Spot position reconstruction for *low-MUs*

Due to treatment fractionation and the use of multiple fields per fraction, proton therapy machines are asked to deliver a very small amount of radiation per spot, resulting in extremely low MUs, generally smaller than 0.5. An analysis of the MU distribution for a sample of patients treated in the same room where the measurements were performed shows that the percentage of spots having MU lower than 0.5 is around 85%. In particular, for the brain case reported in the paper, where the size of the tumor was small, the spot intensity has its highest value at 0.14. For this reason, it is clinically more relevant to estimate the spot position uncertainties in the *low-MU* region.

To reconstruct the spot position at *low-MUs* we extract the information stored in the log-files obtained during *high-MU* irradiations reading the measured spot position that corresponds to the desired low-MU value. Figure 2 shows a sketch of the information recorded in a log-file for an irradiation at 1 MU. This example reconstructs the position

corresponding to 0.1 MU. Summing up the delivered charge till the desired value allows to get the corresponding spot position (x_2, y_2).

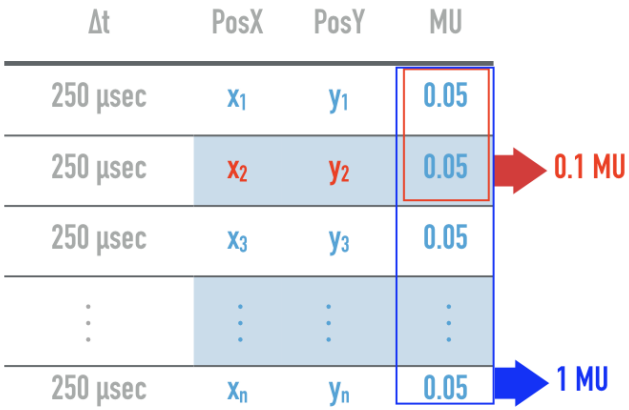

Figure 2. Simplified representation of a machine log-file for an irradiation at 1 MU. The read-out of the ICs is performed every 250 µsec, when the spot position and the delivered charge (a fraction of its final value) are recorded. Summing up the delivered charge till the desired value (0.1 MU in this example) allows to get the corresponding spot position (x_2, y_2).

The spot position obtained with this method is then compared with the corresponding Lynx measurement and the systematic and random shifts are calculated in terms of the mean and standard deviation of the spot position difference.

2.1.3. Test of the methodology for low-MU spot position reconstruction

The method used to reconstruct the spot position at low-MU is valid only under the hypothesis of stability of the delivery, where no systematic drift of the spot position is observed. Under this condition, we can imagine that the spot position measured with the Lynx will not change during the spot irradiation and it can be taken as a reference for all the recorded positions of one spot. To test the methodology, we have reconstructed the spot position at MU = 0.5 from the MU=1 delivery and we have compared with the actual MU=0.5 delivery, for which Lynx measurements were available as well.

2.1.4. Look-up tables

Look-up tables of the mean and standard deviation of the spot position shift as a function of MU, energy and spot position at the isocenter plane have been created to build a model of the uncertainties. Interpolating the look-up tables allows to retrieve the systematic and random uncertainties associated to any of the irradiated spots. For every spot, the position is corrected for the systematic shift using the interpolated mean value and the random error is sampled from a zero-centred normal distribution with the sigma obtained from the interpolation.
Moreover, the spot position and the measurement may depend on the gantry angle. Therefore, we have created a different model for the two measured gantry angles. The results presented here refer to the measurements performed at gantry angle 270˚. Similar results are observed for the measurements at gantry angle 0˚.

2.2. Log-based post-treatment PSQA workflow

Once the plan is delivered to the patient or in a dry-run, where the beam is shot in air, as in our case, the information stored in the machine log-files are used to reconstruct the plan in terms of spot position (Figure 3) and MU. The new plan ($Plan_{LOGS}$) is used to recompute the actual delivered dose with MCsquare ($MC\text{-}DOSE_{LOGS}$) and compared with the planned dose ($MC\text{-}DOSE_{PLAN}$). Different analysis are carried out: comparison of clinical indicators related to different anatomical structures, comparison of dose volume histograms (DVH), gamma index, and statistical analysis on the spot position and MU errors.

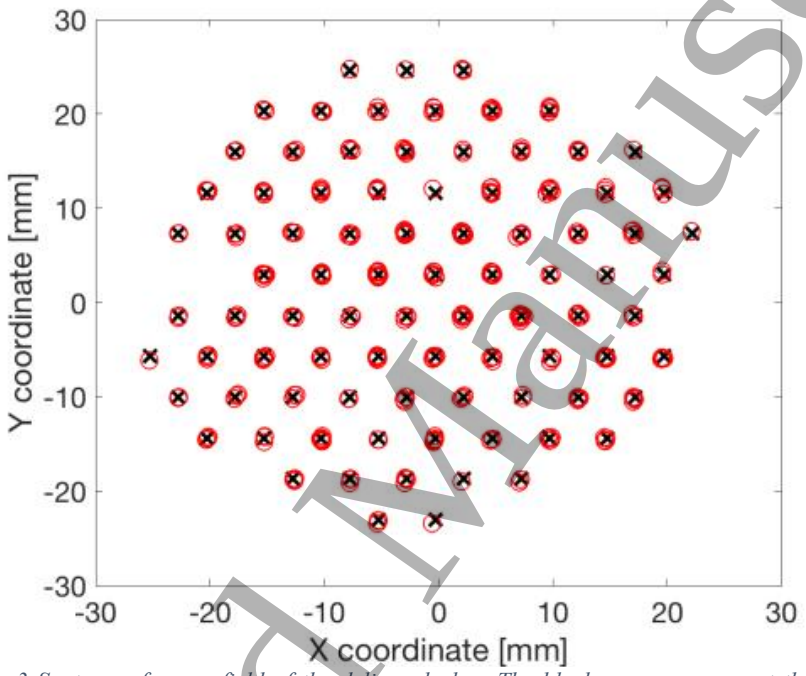

Figure 3 Spot map for one field of the delivered plan. The black crosses represent the planned positions, while the red circles are the reconstructed positions from the machine log-files

A patient treatment plan contains thousands of spots organized in several energy layers, each of them defined by a specific spot position and MU. Therefore, for every spot in the plan it is possible to retrieve the corresponding log-file uncertainty from our model. A flux diagram of the final post-treatment PSQA is shown in Figure 4. As explained before, a comparison between the planned dose ($MC\text{-}DOSE_{PLAN}$) and the log-reconstructed delivered dose ($MC\text{-}DOSE_{LOGS}$) is performed. The log-reconstructed plan is then corrected for the spot-wise systematic uncertainty and spot position uncertainties are sampled, for every spot in this new plan, from a zero-centred normal distribution with sigma values obtained from the interpolation of the look-up tables. These uncertainties are then used to simulate 500 new scenarios, finally represented as a confidence interval around the DVHs allowing to judge the plan delivery accuracy.

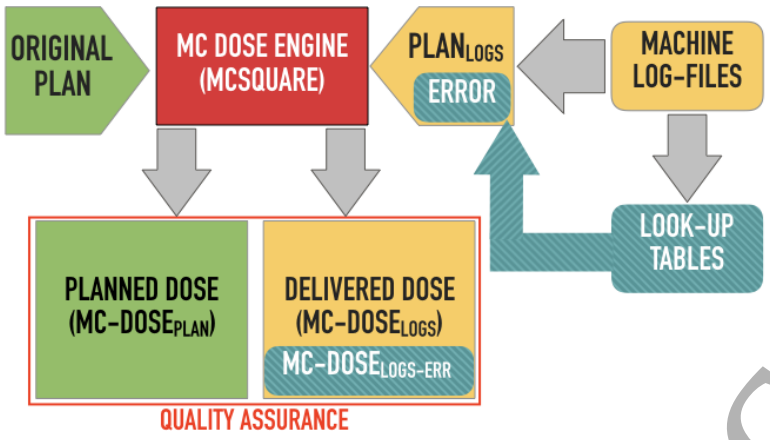

Figure 4 Flux diagram of the post-treatment PSQA. Spot position uncertainties are sampled from the errors in the look-up tables in a spot-wise fashion, and included in the Monte Carlo calculation of the dose.

2.3. Patient case

The model obtained has been tested on a clinical case for a brain patient, delivering one fraction of the treatment plan in the same room used to build the look-up tables.
MIROpt (Barragan et al 2017), an in-house, open source, treatment optimizer based on Monte Carlo dose calculation with MCsquare, was used to generate the treatment plan for the brain patient. The target prescription was set to 59.4 Gy in 33 fractions, and two posterior beams (145˚, 225˚) were used to create the plan. The scanning grid used in MIROpt follows a hexagonal pattern with a lateral spot spacing of 5 mm, and a constant spacing between energy layers of 5 mm-WET (Water Equivalent Thickness). The dose contribution matrix was computed using 10^5 protons per spot, and a final forward dose calculation with 10^7 protons was performed to verify that the plan satisfied the required clinical constrains. The final plan generated by MIROpt was post-processed to delete those spots with MU smaller than 0.02, representing the minimum value deliverable by the IBA system.

3. Results

3.1. Delivery errors

Lynx measurements have been analysed to ensure that the detector was correctly aligned and that no systematic shift was present during the data taking period. This allows to disentangle the delivery errors from the log-file uncertainties. Moreover, the difference observed between the Lynx-measured and planned spot positions are negligible compared with the difference between the log-recorded and the planned/measured spot positions. Figure 5 shows the map-averaged y-position error distributions for an energy of 100 MeV and MU from 0.5 up to 10. Similar values are observed for the x-position error. The three combinations, Plan-Logs, Lynx-Logs, and Lynx-Plan, are shown with the corresponding

standard deviations, 0.57 mm, 0.54 mm and 0.19 mm. The mean values are represented by the dashed lines. The tail present in the Lynx-Logs and Lynx-Plan distributions comes from the outlying spots, since the spot positions recorded in the log-files have a bigger error for spots located at high distance from the center. The effect is not present when looking at the error between plan and Lynx, supporting the hypothesis that it is inherited from the log-file measurements. The measurements performed with the Lynx allow to reach the needed accuracy and they are used as a reference of the actual delivered spot position.

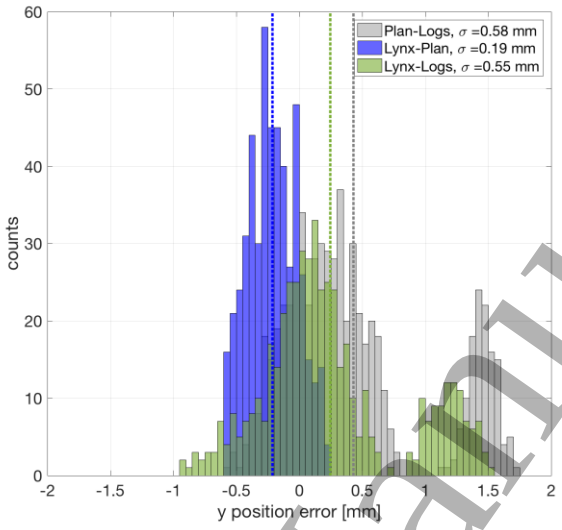

Figure 5 Map-averaged spot position error in the y coordinate between Lynx and plan (blue), Lynx and logs (green) and plan and logs (grey), for an energy of 100 MeV and MU from 0.5 up to 10. The dashed lines show the mean values.

3.2. High-MU spots delivery

Figure 6 shows the mean value (systematic uncertainty) and standard deviation (random uncertainty) of the measured shift in the x-coordinate as a function of the spot number and spot position for an energy of 100 MeV. Different lines correspond to different irradiated MUs. Similar behaviours are observed for the other energies.

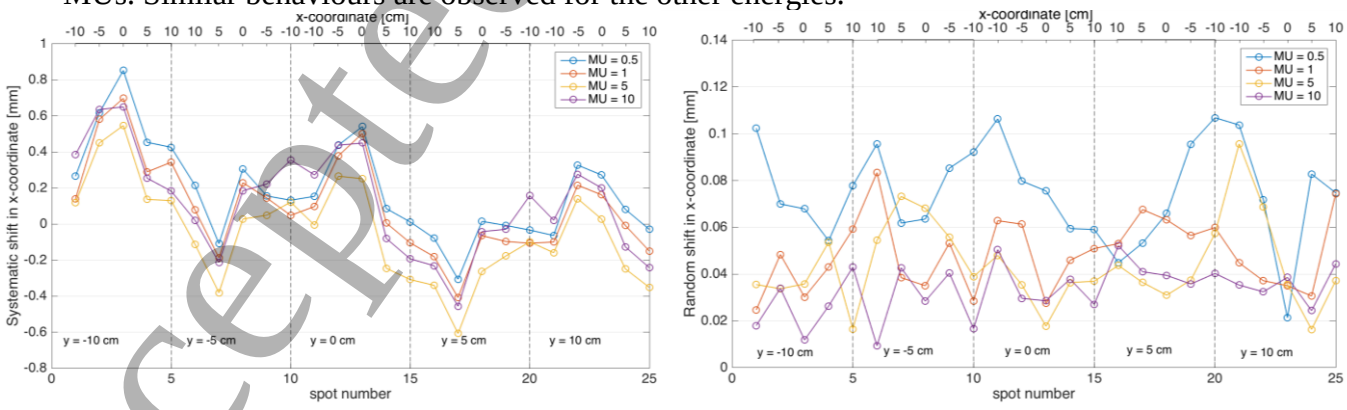

Figure 6 Systematic (left) and random (right) uncertainties in the x-coordinate as a function of the spot number (bottom x-axis) at 100 MeV. Different lines correspond to different MU values. The upper x-axis shows the x-coordinate position. The vertical lines indicate the change in the y-coordinate.

The observed systematic shift is strongly dependent on the spot position and can reach values of ± 1 mm in the x direction, and up to 1.5 mm in the y direction. The random shift in both direction remains below 0.2 mm, confirming that the log-file measurements are extremely precise.

3.3. Test of the low-MU reconstruction method

Figure 7 (left) shows the measured spot positions of the central spots, for two deliveries at MU = 0.5 and MU = 1, together with the planned position. The right panel of the same Figure shows the distribution of the difference between the recorded and the Lynx-measured x-position for MU = 0.5 (blue) and MU = 0.5 reconstructed from MU = 1 (green). A comparison of the two data sets was done using a two-sample F-test, where the test statistics is the ratio between the variances of the two samples. The null hypothesis is that the two data sets come from populations having the same variance. The test confirms the null hypothesis with a p-value of 0.3. The same test has been repeated for several combinations of data sets, where the delivery at MU = 0.5 has been reconstructed using MU = 5, 10, and at different energies. All tests performed confirm the null hypothesis with p-values ranging from 0.3 up to 0.9. The reconstruction method can be used to estimate the error uncertainties for the low-MU regime where measurements are missing.

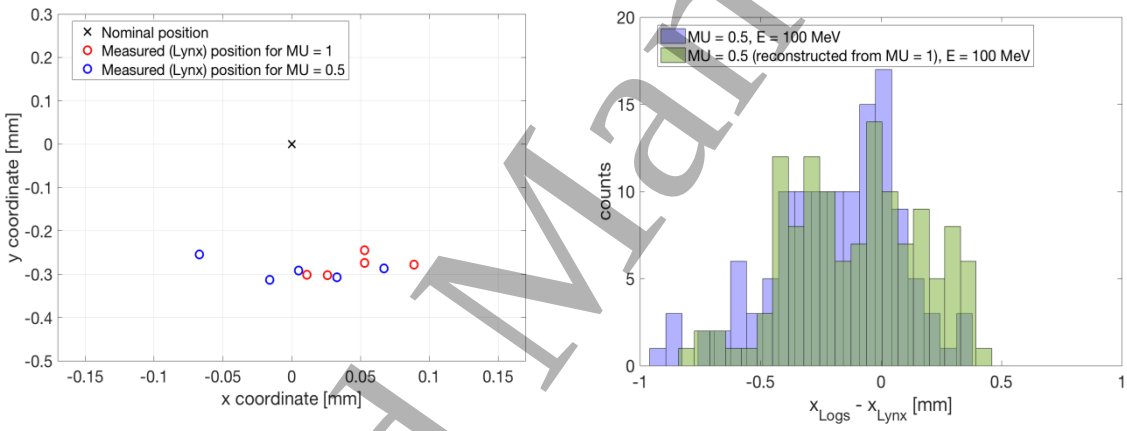

Figure 7 Left: Spot position for the central spot measured with Lynx for MU=0.5 and MU = 1. The plot shows the stability of the delivery. Right: Distribution of the difference between the x-position recorded in the log-files and the Lynx measurements for E = 100 MeV. The blue histogram represents the distribution obtained from the MU = 0.5 delivery, while the green histogram is the distribution obtained when MU = 0.5 is reconstructed from the MU = 1 delivery.

3.4. Low-MU reconstructed spots

Using the irradiations at high-MUs we have estimated the systematic and random position uncertainties for low-MUs. Figure 8 shows an example of the mean values and standard deviations of the measured shift in the x-coordinate at 100 MeV. The curves correspond to 0.04, 0.1, 0.2, 0.3, and 0.4 MU.

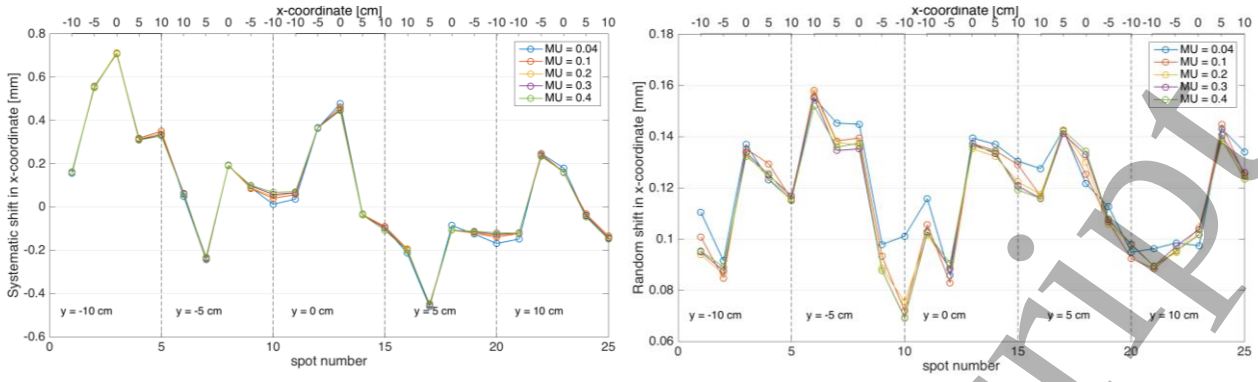

Figure 8 Systematic (left) and random (right) uncertainties in the x-coordinate as a function of the spot number (bottom x-axis) at 100 MeV. Different lines correspond to different MU values reconstructed from the high-MUs irradiations. . The upper x-axis shows the x-coordinate position. The vertical lines indicate the change in the y-coordinate.

The results show that the spot positions in the low intensity region can be reconstructed with an accuracy of ±1 mm in the x direction, and up to +1.5 mm in the y direction, and a precision within 0.2 mm in both directions, similarly to what has been observed for the high-MU irradiations.

3.5. Patient case

One fraction of the treatment plan was delivered in the same room as the one used to create the model. The irradiation log-files were analysed to test our post-treatment PSQA protocol. The planned and delivered dose were computed simulating 10^8 protons with MCsquare, with an average statistical uncertainty of 0.9% across all the voxels receiving a dose exceeding 0.2 Gy (0.3% uncertainty on average inside the PTV contour).

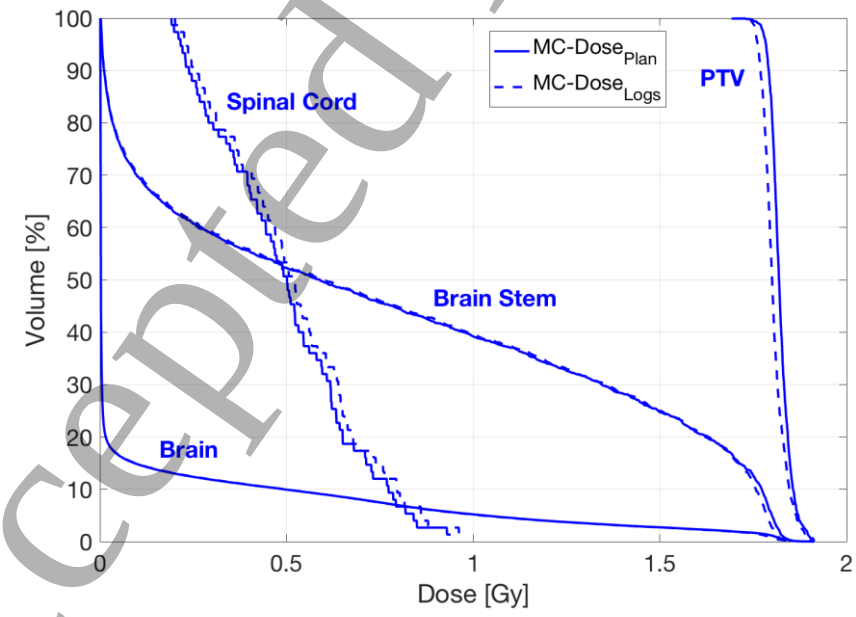

Figure 9 Comparison of DVHs for MC-Doses calculated for the original plan (solid) and the log-reconstructed (dashed) for the PTV region and 3 organs at risk.

Figure 9 shows the comparison of DVHs for the MC-Dose calculated from the original and log-reconstructed plans within the PTV contour and three organs at risk. The mean dose difference observed in the PTV region is around 1%. To separate the contribution of the spot-position from the MU log-measurements we have reconstructed the plan using only the log-recorded MUs ($Plan_{LogsMU}$) or the log-recorded positions ($Plan_{LogsPos}$). Figure 10 shows the DVHs for the MC-Doses calculated from the original plan and the three log-reconstructed plans. Our results indicate that the spot position represents the bigger source of error, while the uncertainty for the MU reconstruction has a lower impact on the reconstructed plan.

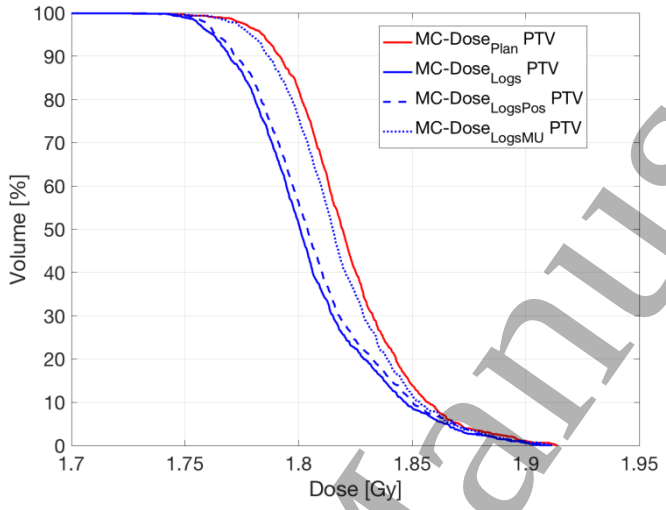

Figure 10 Comparison of DVHs for MC-Doses calculated for the original (red) and the log-reconstructed (blue) plan in the PTV region. The delivery has been reconstructed using the information from the irradiation log files in three different ways: MU-only (dotted blue), spot position only (dashed blue) and both MU and spot position (solid blue).

Figure 11 shows the spot positions for the new plans obtained from the log-reconstructed plan corrected for the systematic uncertainties when adding a reconstruction error from the random uncertainties in the model.

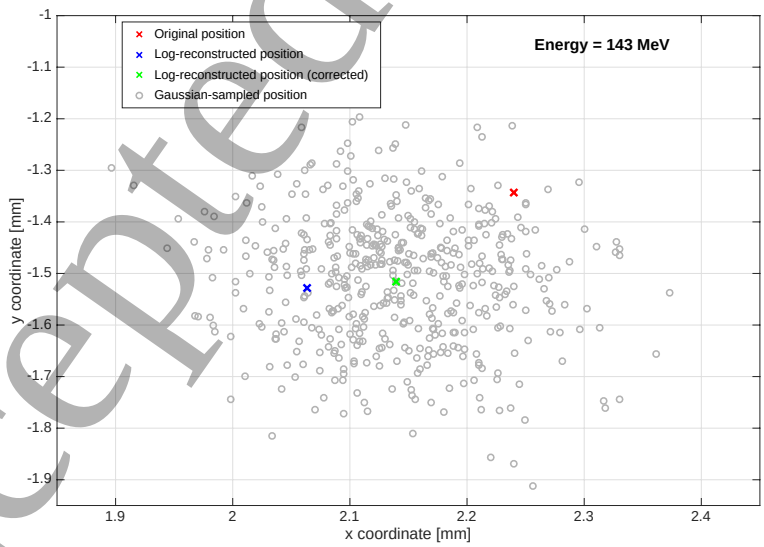

Figure 11 Position of one of the irradiated spot from the original plan (red), the log-reconstructed plan (blue), the log-reconstructed plan corrected for the systematic uncertainties (green) and 500 new scenarios obtained sampling the error from a Gaussian distribution centred at 0 and sigma obtained from the random uncertainties (grey).

Figure 12 shows the DVHs for the planned and the reconstructed dose with the inclusion of the error band calculated from the log-file random uncertainties. The reconstructed dose is corrected for the systematic uncertainty and the 500 new plans including the random uncertainties are used to generate the 95% confidence interval.

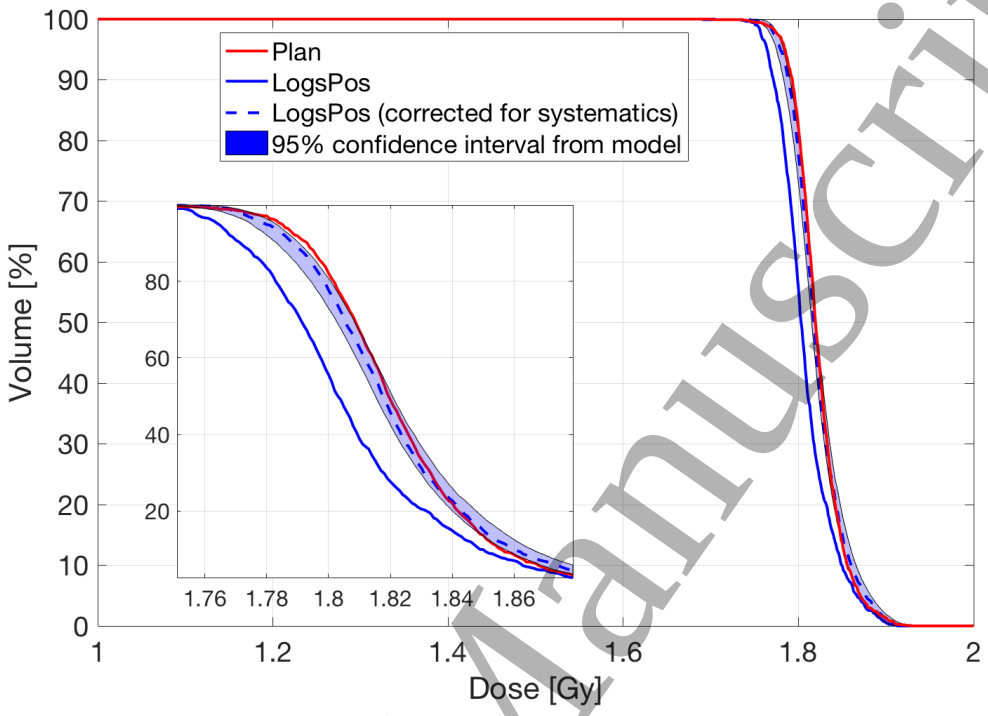

Figure 12 Comparison of DVHs for the dose inside the PTV region. MCsquare is used to estimate the planned dose (red) and the log-reconstructed dose (blue). The delivery has been reconstructed using the information from the irradiation log-files using the spot position only, and the planned MUs (solid line). The reconstructed plan is corrected for the systematic uncertainties (dashed line). The blue band is the 95% confidence interval obtained from the model (random uncertainties only). The inner panel shows an inset of the central region.

4. Discussion

The analysis of the log-file data and the comparison between the planned and delivered (reconstructed) dose per fraction indicate that the spot position measurement done by the proton therapy machine is less accurate than the actual delivered spot position, since the beam is delivered within an accuracy of less than 0.2 mm, while the systematic uncertainty from the log-file measurements can reach values up to 1.5 mm in some cases. The dose difference comes essentially from the spot position measurements, while almost no effect is observed when using the irradiated MUs and maintaining the planned position to reconstruct the plan (Figure 10). Therefore, the estimation of the log-position uncertainties and their inclusion in the final dose difference assessment is necessary, since any significant deviation from the original plan might be misinterpreted as a problem in the treatment delivery if no estimation of the expected reconstruction error is included.

Figure 12 includes the estimation of these uncertainties in the DVH representation of the planned and delivered dose within the PTV contour. We observe that the mean dose relative error between the plan and the log-reconstructed dose, originally around 1%, is reduced to

almost zero when the log-reconstructed plan is corrected for the systematic shift and the random errors are included. We observe that the relevant correction comes from the treatment of the systematic shift only. The error band from the random uncertainties is added here for completeness, since for other systems may be significant; but it may be omitted in the final workflow to speed up the pipeline in a case where this is found to be negligible.
The log-reconstructed dose using the spot position only (LogPos) is compatible with the planned dose, indicating that the observed difference is essentially coming from the spot position uncertainties, assuring a high quality of the delivery. An alert on the workflow will trigger additional checks in the opposite case of a reconstructed dose falling outside the error band. However a minor delivery error cannot be entirely excluded, and a certain level of tolerance should be defined in clinical practice for these cases. These levels of tolerance can be established from user-experience and recommended guidelines, as it is typically the case in QA practice.

The model presented in this paper has been obtained from the analysis of hundreds of machine log-files corresponding to the irradiation of a square spot-pattern to explore the effect of the MUs and energy change on the spot position uncertainties. However, additional measurements, including a wider range of the explored parameters, are needed to perform better interpolations and refine the model. During the experiment, measurements were performed only at two gantry angles (0˚, 270˚) preventing us to use interpolation techniques to calculate the uncertainties at the actual treatment beam angles (145˚, 225˚). During the analysis, we tested the two models extracted from the measurements at the two gantry angles and no significant differences were observed. Nonetheless, the dependency, if any, of the spot position uncertainties with the gantry angle needs to be included in the model for completeness.
In addition to this, measurements of the low-MU deliveries are still missing and need to be addressed. As already explained, the Lynx detector used to measure the delivery in our experiment has no sensitivity to low-MU irradiations. Unfortunately, there were no other detectors available at the proton therapy center with the same position resolution as the Lynx and sensitive enough to measure in the low-MU region. In this work, we bypassed the problem reconstructing the spot position and their uncertainties from the high-MU deliveries. The methodology works if we assume that the spot position measured by the Lynx does not change during the time of the spot irradiation, meaning that the delivery is stable within that time frame. To test such a hypothesis we have studied the stability of the spot position from the IC measurement recorded in the log-files, looking at the variation of the measured value during the spot-irradiation. The results show that the spot position measurement is stable within +/- 0.1 mm (one standard deviation), leading to the reasonable conclusion that the delivery is stable.
Another way to address this problem could be to irradiate a plan using the re-painting mode, in such a way to have a high-MU spot delivered in several low-MU spots with the same position and energy. The final irradiation will be measurable by the Lynx and the machine log-files will store the information of such a kind of delivery in several sub-layers, characterized by low-MU spots. Even in such a case where no manipulation of the log-file data is needed to extract the information on the low-MU irradiation, the hypothesis of stability should hold true.
As stressed since the beginning, the model implemented in this work is limited to the estimation of the spot position uncertainties. A complete LogQA should include the modelling of the MU uncertainties as well, although they are expected to be negligible in a first approximation. Therefore, absolute dosimetry measurements should be performed using a dedicated detector, e.g a large area ionization chamber (Gomà et al 2017), to set the reference dosimetry and estimate the MU uncertainties of the machine log-files.

It is worth to mention that machine log-files do not store any information about the irradiated energy, needed for a full reconstruction of the dose. Although regular QA will always be performed to ensure that a beam with the requested energy is correctly delivered, additional external detectors, such as the prompt gamma camera prototype from IBA (Smeets et al 2012), may be beneficial to perform in-vivo dosimetry (Toscano et al 2018, Xie et al 2017) within our new PSQA protocol.
Being room-specific, the LogQA as implemented in our workflow should be envisaged as a part of the room commissioning at first. Moreover, more measurements should be performed during the monthly machine QA to improve the model and guarantee its stability over time. The implementation and maintenance of such a model in clinic is essential for a correct execution of our PSQA protocol.
Finally, the numbers presented in this paper are expected to improve in the future, thanks to several technological advances of the new IBA machines allowing for a better fit accuracy, which is related to the spot position uncertainties estimation.

5. Conclusions

The new PSQA protocol described in this work addresses the problem of finding a fast and more comprehensive method to assure the quality of the delivery for scanned proton therapy. The strong and still growing interest from the community to use the machine irradiation log-files confirms the power of these tools. The information stored in the log-files can be used together with Monte Carlo computations to assess the dose delivered during treatments, and the way to use them have been subject of several recently published works. Nevertheless, to our knowledge, the problem of the estimation of the log-file measurement uncertainties has not been addressed yet and we believe to be of utmost importance for the final implementation of a PSQA workflow in clinic.
In the proposed PSQA, the quality of the TPS calculation in patient anatomy and its sensitivity to treatment uncertainties (Lin et al 2016, Unkelback et al 2009, Paganetti 2012, Brousmiche et al 2017) can be verified with our independent Monte Carlo dose calculation (pre-treatment PSQA). The delivered dose can be reconstructed after every treatment fraction using the information stored in the machine log-files and the secondary dose engine to check the quality of the delivered treatment (post-treatment PSQA). Moreover, the inclusion of the LogQA during the commissioning period and as a part of the machine QA will allow to characterize the machine log-file uncertainties. With the inclusion of the log-file uncertainties in the dose calculation we expect to get a better assessment of the quality of the treatment plan delivery and a more realistic estimation of acceptable plans. In conclusion, our new protocol can assure a fast PSQA, an essential requirement for the implementation of an online adaptive radiation therapy strategy in the clinics.

6. Acknowledgment

S. Toscano and A. Barragán Montero are funded by Fonds Baillet-Latour. K. Souris is supported by a research grant from Ion Beam Application (IBA s.a., Louvain-la-Neuve, Belgium).

References

Barragán Montero AM, Souris K, Sanchez-Parcerisa D, Sterpin E, Lee JA 2018 Performance of a hybrid Monte Carlo-Pencil Beam dose algorithm for proton therapy inverse planning *Medical Physics* **45** 846-862

[Belosi MF, van der Meer R, Garcia de Acilu Laa P, Bolsi A, Weber DC, Lomax AJ 2017 Treatment log files as a tool to identify treatment plan sensitivity to inaccuracies in scanned proton beam delivery *Radiotherapy and Oncology* **125** 514–519.

Brousmiche S, Souris K, de Xivry JO, Lee JA, Macq B, Seco J 2017 Combined influence of CT random noise and HU-RSP calibration curve nonlinearities on proton range systematic errors *Physics in Medicine and Biology* **62** 8226-8245
Gomà C, Safai S, Vörös S 2017 Reference dosimetry of proton pencil beams based on dose-area product: a proof of concept. *Phys Med Biol* **62** 4991-5005

Grevillot L, Bertrand D, Dessy F, Freud N, Sarrut D 2011 A Monte Carlo pencil beam scanning model for proton treatment plan simulation using GATE/GEANT4. *Phys Med Biol* **56** 5203–19

Lin L et al 2016 Evaluation of motion mitigation using abdominal compression in the clinical implementation of pencil beam scanning proton therapy of liver tumors *Medical Physics* **44** 703-712

Lomax AJ 1999 Intensity modulated methods for proton therapy *Phys. Med. Biol.* **44** 185–205

Low DA, Harms WB, Mutic S, and Purdy JA 1998 A technique for the quantitative evaluation of dose distributions, *Med. Phys*. **25** 656

Meier G, Besson R, Nanz A, Safai S, Lomax A 2015 Independent dose calculations for commissioning, quality assurance and dose reconstruction of PBS proton therapy *Phys Med Biol*. **60** 2819–2836.

Paganetti H, 2012 Range uncertainties in proton therapy and the role of Monte Carlo simulations", *Phys. Med. Biol.* **57** R99–R117

Scandurra D, Albertini F, van der Meer R, Meier G, Weber DC, Bolsi A, Lomax A 2016 Assessing the quality of proton PBS treatment delivery using machine log files: comprehensive analysis of clinical treatments delivered at PSI Gantry 2 *Phys. Med. Biol.* **61** 1171

Smeets J et al 2012 Prompt gamma imaging with a slit camera for real-time range control in proton therapy *Phys. Med. Biol.* **57** 3371

Souris K, Lee JA, Sterpin E 2016 Fast multi-purpose Monte Carlo simulation for proton therapy using multi- and many-core CPU architectures *Med Phys* **43** 1700–12.

Toscano S, Souris K, Sterpin E, Janssens J, Petzoldt J, Vander Stappen F, Smeets J, Geets X, Teo K 2018 From range measurements to dose: in-vivo dosimetry using the prompt gamma camera *ESTRO 37 (20-24 April, Barcelona, Spain)*

Unkelbach J, Bortfeld T, Martin BC, Soukup M 2009 Reducing the sensitivity of IMPT treatment plans to setup errors and range uncertainties via probabilistic treatment planning *Medical physics* **36** 149-163

Xie Y et al 2017 Prompt gamma imaging for *in vivo* range verification of pencil beam scanning proton therapy *Radiation Oncology* **99** 210-218

Zhu X et al 2011 Patient-specific quality assurance for prostate cancer patients receiving spot scanning proton therapy using single-field uniform dose *Int. J. Radiat.Oncol. Biol. Phys.* **81** 552–9.

Zhu X et al. 2015 Towards Effective and Efficient Patient-Specific Quality Assurance for Spot Scanning Proton Therapy, *Cancers* **7** 631-647